Herpes Simplex Virus gE/gI and US9 Proteins Promote Transport of both Capsids and Virion Glycoproteins in Neuronal Axons[▽]

Aleksandra Snyder,[1] Katarina Polcicova,[2] and David C. Johnson[1]*

Department of Molecular Microbiology and Immunology, Oregon Health and Sciences University, Portland, Oregon 97239,[1] and Institute of Virology, Slovak Academy of Sciences, Bratislava, Slovak Republic[2]

Following reactivation from latency, alphaherpesviruses replicate in sensory neurons and assemble capsids that are transported in the anterograde direction toward axon termini for spread to epithelial tissues. Two models currently describe this transport. The Separate model suggests that capsids are transported in axons independently from viral envelope glycoproteins. The Married model holds that fully assembled enveloped virions are transported in axons. The herpes simplex virus (HSV) membrane glycoprotein heterodimer gE/gI and the US9 protein are important for virus anterograde spread in the nervous systems of animal models. It was not clear whether gE/gI and US9 contribute to the axonal transport of HSV capsids, the transport of membrane proteins, or both. Here, we report that the efficient axonal transport of HSV requires both gE/gI and US9. The transport of both capsids and glycoproteins was dramatically reduced, especially in more distal regions of axons, with gE⁻, gI⁻, and US9-null mutants. An HSV mutant lacking just the gE cytoplasmic (CT) domain displayed an intermediate reduction in capsid and glycoprotein transport. We concluded that HSV gE/gI and US9 promote the separate transport of both capsids and glycoproteins. gE/gI was transported in association with other HSV glycoproteins, gB and gD, but not with capsids. In contrast, US9 colocalized with capsids and not with membrane glycoproteins. Our observations suggest that gE/gI and US9 function in the neuron cell body to promote the loading of capsids and glycoprotein-containing vesicles onto microtubule motors that ferry HSV structural components toward axon tips.

Alphaherpesviruses have evolved specialized mechanisms to facilitate their long-distance travel both in epithelial tissues and in the nervous system (10, 24, 45). The spread of alphaherpesviruses from latently infected neurons following reactivation involves the transport of virus particles from the neuronal-cell body along axons to axonal termini and transfer across junctions formed between neurons and epithelial cells. This anterograde transport in axons apparently involves kinesin motors that move virus particles along microtubules toward axon termini (26, 30, 34). Two models currently describe this transport (1, 7, 10, 26, 30, 34, 36, 39, 41–43, 45). The Separate model suggests that viral capsids are transported on microtubule motors separately from lipid vesicles containing viral envelope glycoproteins, with viral envelopment occurring at axon termini. This model is supported by electron microscopic studies showing herpes simplex virus (HSV) nonenveloped capsids in transit in distal segments of axons (35, 36, 39). Moreover, antibody-staining studies involving HSV and the pig pseudorabies virus (PRV) demonstrated antibody-stained capsids to be separate from vesicles stained with viral-membrane glycoprotein-specific antibodies (19, 35, 41–43). Additionally, HSV capsids labeled with a fluorescent fusion protein were separate from antibody-stained glycoproteins in axons, and a glycoprotein gD fusion protein was separate from antibody-stained capsids (42, 43). The Married model suggests that alphaherpesvirus capsids acquire an envelope containing viral glycopro-

teins in the neuron cell body and that enveloped virions are subsequently transported to axon tips within transport vesicles. Electron microscopic studies showed PRV capsids surrounded by membrane vesicles during anterograde transport (7, 17). Further, live-cell imaging of a PRV recombinant expressing a dually fluorescent capsid protein and glycoprotein showed extensive overlap of these signals, providing strong support for the transport of enveloped virions (1). Certain of the studies do not discount a third possibility in which alphaherpesvirus capsids are transported within cell-derived transport vesicles that do not contain the viral-membrane glycoproteins (29).

HSV and PRV express two proteins, a heterodimeric membrane protein, gE/gI, and US9, that play important roles in virus spread in epithelial and neuronal tissues (reviewed in references 24 and 45). gE/gI and US9 facilitate spread, at least in part, by promoting intracellular sorting of nascent HSV and PRV in epithelial (gE/gI) and neuronal (gE/gI and US 9) cells. Thus, studies of gE/gI and US9 have great potential for shedding light on the poorly understood and much debated process of alphaherpesvirus anterograde transport in neuronal axons.

HSV and PRV with mutations in either subunit of the gE/gI dimer exhibit major defects in virus spread in both epithelial and neuronal tissues (11–13, 21, 25, 38, 46, 49). Based on imaging and mutational analyses of HSV gE and gI mutants in cultured epithelial cells, we proposed a molecular model for how gE/gI facilitates epithelial cell-to-cell spread (24, 38). In this model, HSV gE/gI promotes virus assembly into subcompartments of the trans-Golgi network (TGN), so that newly enveloped virions become sorted to cell junctions rather than to apical surfaces. This directed sorting of viral particles promotes more efficient virus spread to neighboring cells. Both the cytoplasmic (CT) and the extracellular (ET) domains of gE/gI

play important roles in this cell-to-cell spread, with the CT domain promoting distribution of virus particles to epithelial cell junctions and the ET domain promoting transfer across cell junctions (9, 25, 38, 47, 48). Less is known about how gE/gI promotes virus spread in the nervous system, but it was found that HSV gE$^-$ and gI$^-$ mutants displayed markedly reduced anterograde spread between neurons within the retina and from the retina to retinorecipient regions of the brain (12, 46) in the nervous systems of animals. Additionally, Ch'ng et al. (6, 7) demonstrated that PRV gE/gI is required for efficient anterograde transport of both capsids and glycoproteins in cultured rat neurons. While it appears likely that HSV gE/gI promotes the transport of viral structural components in neuronal axons, it is not clear whether capsid or membrane protein transport, or both, is affected.

The HSV and PRV US9 proteins function in the nervous system to promote anterograde spread (3, 4, 38). However, unlike gE/gI, HSV US9 does not obviously promote virus spread in cultured epithelial cells or epithelial tissues (38). In epithelial cells or tissues, an HSV US9-null mutant replicated and spread normally. Moreover, US9-HSV spread into neurons in the retrograde direction and replicated normally in the neurons. However, the US9$^-$ mutant was severely inhibited in the anterograde spread from ganglia to the cornea (38). Similarly, PRV US9 mutants either lacking US9 or with mutations in US9 TGN trafficking motifs displayed reduced anterograde spread from the retina to retinorecipient regions of the brain (3, 4). Therefore, US9 appears to function exclusively in neurons to promote virus spread. Studies of how PRV US9 facilitates anterograde transport in cultured neurons initially concluded that US9 promotes the transport of viral glycoproteins, but not the transport of capsids, in axons (44, 45). However, more recently, studies from the same laboratory found that US9$^-$ mutants were defective for both capsid and glycoprotein transport in axons. Using a mouse retina model of HSV infection, LaVail et al. (27) concluded that HSV US9 was required for the transport of capsids, but not viral glycoproteins, from the retina into the optic nerve.

Initial studies examining HSV US9 described the protein as part of the viral tegument (18). More recent studies indicated that HSV US9 is found associated with the endoplasmic reticulum and Golgi apparatus, as well as with cytoplasmic, unenveloped capsids (27). On the other hand, detailed studies of PRV US9 demonstrated that US9 is a type II membrane protein associated with Golgi or perinuclear membranes (2). Both the HSV and PRV US9 proteins contain C-terminal hydrophobic sequences that appear to be membrane-anchoring domains, as well as N-terminal CT domains containing TGN sorting motifs, including tyrosine and dileucine motifs and a cluster of acidic residues adjacent to phosphorylation sites. These TGN sorting motifs were required for PRV US9 function (2, 4). Tomishima and Enquist and Tomishima et al. (44, 45) suggested that US9 might act as a molecular tag on the cytoplasmic surfaces of membrane vesicles containing viral glycoproteins to tether the vesicles onto microtubule motors. Whether this model applies to HSV axonal transport has not yet been determined.

Exactly how HSV gE/gI and US9 promote virus egress in neurons is not clear. All of the published evidence for HSV is consistent with the Separate model. HSV gE/gI is a membrane protein, and HSV US9 may also be membrane bound. It is important to determine whether these membrane proteins, if this is the case, can affect the separate transport of membrane glycoproteins, as well as capsids (which might not be associated with membranes). Here, we report that HSV US9$^-$, gE$^-$, and gI$^-$ mutants all display defects in both capsid and glycoprotein transport into axons. We also made surprising observations that US9 was colocalized with capsids that were being transported in axons and not with viral-membrane glycoproteins. In contrast, gE/gI was colocalized with glycoproteins and not with capsids. Together, these studies contribute to models showing how HSV is transported in axons and begin to describe how gE/gI and US9 might promote this transport.

MATERIALS AND METHODS

Cells and viruses. Vero and human R970 cells were grown in Dulbecco's modified Eagle's medium containing 7% fetal bovine serum. The wild-type HSV type 1 (HSV-1) strain F and FgE/GFP (14), FgE/GFP-R, F-US9/GFP (37), FUS9/GFP-R (37), F-gEΔCT (47), F-gI/GFP, FgI/GFP-R, F-US9-HA, F-VP26-GFP (43), and SC16-gD-YFP (42) were propagated and their titers were determined on Vero cells.

Cultured neurons. Human SK-N-SH neuroblastoma cells were purchased from the American Type Culture Collection (Rockville, MD) and propagated in growth medium as described previously (43). SK-N-SH cells were differentiated to induce axons with retinoic acid as described previously (43). Cultured neurons were infected with the HSV wild type and mutants after 7 to 10 days of this differentiation. The neurons were infected with various viruses for either 18 or 24 h and then fixed, permeabilized, and stained with various antibodies.

Construction of HSV gE-repaired and gI mutant viruses. A repaired version of the gE$^-$ mutant F-gE/GFP was constructed by preparing viral DNA from F-gE/GFP-infected Vero cells by sodium dodecyl sulfate lysis and phenol-chloroform extraction and cotransfecting this DNA and plasmid pUC US7/8 (47) linearized with XmnI into Vero cells by using the calcium-phosphate transfection technique (47). The plaques were screened for loss of green fluorescent protein (GFP). To construct a gI-null HSV, the gI gene was replaced with GFP sequences linked to the human cytomegalovirus immediate-early promoter (pEGFP-Cl; Clontech). A PCR-derived fragment of the human cytomegalovirus/GFP sequences was digested with NcoI and AgeI and inserted into plasmid pUC19 gI (containing the US7 gI gene), which was also digested with NcoI and AgeI. The pUC19gI-GFP plasmid was sequenced, linearized with XmnI, and cotransfected with wild-type HSV strain F DNA into Vero cells using the calcium phosphate transfection technique. The plaques were screened for the presence of GFP, and the recombinant was denoted F-gI/GFP. To construct a repaired version of F-gI/GFP, F-gI/GFP DNA was prepared and cotransfected with plasmid pUC19gI (containing the wild-type gI gene) that was linearized with XmnI into Vero cells using Lipofectamine. The plaques were screened for loss of GFP, and the virus was denoted F-gI/GFP-R. In all cases, viruses were plaque purified three times.

Construction of an HSV recombinant expressing an epitope-tagged US9 protein. An HSV strain expressing a US9 protein modified by the addition of a 9-amino-acid influenza virus hemagglutinin (HA) epitope (encoded by the added DNA sequence 5′-TAC CCA TAC GAT GTT CCA GAT TAC GCT-3′) inserted directly after the initiation codon was constructed and denoted F-US9-HA. A two-step PCR protocol was used. The first set of reactions contained the pUC US7/8/9 (37) plasmid with either (i) the sense oligonucleotide CTGTGTG GGATTGCGTGGTATGTGACGT**CAATTG**CCCGAGGCGCATAAAG (containing sequences corresponding to the upstream region of the start site of US9 with an MfeI restriction site [boldface] incorporated into the primer) and (ii) the antisense oligonucleotide AGCGTAATCTGGAACATCGTATTGGTAC*ATC GAGGCCGGAAGAAAGCTCC* (containing sequences corresponding to the US9 sequence and the ATG start site, followed by an HA tag sequence [in italics]) or (iii) the sense oligonucleotide ATG*TACCAATACGATGTTCCAGA TTACGCT*ACGTCCCGGCTCTCCGATCC (containing sequences corresponding to the ATG start site of US9 and an HA tag sequence [italics] and downstream sequence of US9 from the start site) and (iv) the antisense oligonucleotide CTATGACCATGATTACGCC**AAGCTT**TAGCGGGAGCAGCCACATCAGG AGCG (containing sequences corresponding to the 3′ end of the US9 gene with a HindIII restriction site [boldface] incorporated into the primer). The two separate PCR products from this first set of reactions were diluted, mixed, and

subjected to PCR amplification using the following oligonucleotides: CTGTGT GGGGATTGCGTGGTATGTGACGT**CAATTG**CCCGAGGCGCATAAAG and CTATGACCATGATTACGCC**AAGCTT**TAGCGGAGCAGCCACATCA GGAGCG (boldface sequences represent MfcI and HindIII restriction sites, respectively, incorporated into each primer). This second PCR produced a 430-bp PCR fragment corresponding to the US9 gene with the addition of the HA epitope sequences inserted directly following the methionine start site of US9. This PCR fragment was subcloned into pCR2.1 TOPO and sequenced. The US9-HA sequences were removed by using MfeI and BbvCI and inserted into pUC US7/8/9 (37) that had been digested with MfeI and BbvCI. pUC-US7/8/9 containing the US9-HA fusion was digested with XmnI and cotransfected with HSV F-US9/GFP DNA using calcium phosphate precipitation (11). The viruses were screened for loss of GFP, and a virus that expressed US9-HA was plaque purified three times.

Radiolabeling of infected cells and immunoprecipitation. R970 cells were infected with HSV at 10 PFU/cell for 6 h, and the cells were washed extensively in medium lacking methionine and cysteine and labeled for 3 h in medium lacking methionine and cysteine with [^{35}S]methionine/cysteine (Amersham) (50 Ci/ml). The cells were suspended in NP-40/deoxycholate lysis buffer (100 mM NaCl, 50 mM Tris-HCl [pH 7.5], 1.0% NP-40, 0.5% deoxycholate) supplemented with 2 mg of bovine serum albumin/ml and 1 mM phenylmethylsulfonyl fluoride, and the extracts were frozen at 70°C. HSV-1 gD was immunoprecipitated by using monoclonal antibody (MAb) DL6, gE was precipitated by using MAb 3114, and gI was precipitated by using MAb 3104. The immunoprecipitated cell extracts were eluted by boiling them in buffer containing 2% sodium dodecyl sulfate, 2% β-mercaptoethanol and subjected to electrophoresis as described previously (47).

Antibodies. Rabbit polyclonal antiserum specific for gD (rabbit no. 45) was kindly provided by Gary Cohen and Roselyn Eisenberg (University of Pennsylvania, Philadelphia), and rabbit polyclonal anti-gB serum (rabbit no. 63) specific for gB was kindly provided by Pat Spear (Northwestern Medical School, Chicago, IL); both were used at 1:1,000. Rabbit polyclonal serum and a mouse MAb specific for the HA epitope were obtained from Zymed Laboratories and used at 1:100. Mouse MAb ICP5 (Virusys, North Berwick, ME) and H1.4 (Biodesign International, Sato, ME) specific for HSV capsid protein VP5 were mixed together and used at 1:500. Rabbit polyclonal antiserum specific for HSV-1 US9 (37) was generated as follows. Peptide MTSRLSDPNSSARSDMSVPC was synthesized by Resgen Invitrogen Corp., coupled to keyhole limpet hemocyanin, and used to immunize rabbits as described previously (20). Antibodies from two rabbits were pooled, diluted to 1:500, and serially adsorbed onto fixed and permeabilized uninfected SK-N-SH neurons. The adsorbed antibodies were further purified by adsorption onto the US9 peptide coupled to SulfoLink (Thermo Scientific) according to the manufacturer's instructions.

Immunofluorescence microscopy of HSV-infected neurons. Neurons were infected with HSV using 1 to 3 PFU/cell and incubated for 18 to 24 h at 37°C in differentiation medium. The neurons were fixed, permeabilized, and stained with various anti-HSV mouse, rat, or rabbit antibodies, followed by secondary antibodies as described previously (43). The cells were mounted on glass slides using Fluormount G (Southern Biotech, Birmingham, AL). Immunofluorescence microscopy, followed by deconvolution, was performed in the Oregon Health and Sciences University Molecular Microbiology and Immunology Research Core Facility. Images were acquired on the Olympus IX71 microscope (differential interference contrast) equipped with DeltaVision software as described previously (43). Eleven 0.2-μm *xy* sections were obtained in two-color images and deconvolved as described previously (43). Background immunofluorescence was quantified using uninfected controls (usually 200 light units) and compared to the fluorescence light units exhibited by specific antibodies in HSV-infected cells. Only samples exhibiting light intensities ≥2.5-fold higher than background were used for analysis. In determining colocalization of puncta, high-resolution images were used to reveal individual pixels of 0.2 μm, and the distribution of pixels (whether concentric or nonconcentric) in two dimensions was photographed. Further, three-dimensional images of colocalized puncta were generated by stacking 11 *xy* sections obtained for each image to generate a *z* stack. In these three-dimensional images, the voxel (volumetric pixel) sizes were 0.14 μm in the *xy* plane and 0.2 μm in the *xz* plane. The three-dimensional images were rotated and examined for puncta overlap in all directions. Images that exhibited yellow fluorescence (overlap of green and red fluorescence) throughout the rotation were defined as colocalizing. No pixel shift occurs between colors in this system.

Quantification of capsid and glycoprotein puncta in HSV-infected SK-N-SH neuronal axons. Differentiated SK-N-SH neurons exhibit axons of 25 μm to 75 μm. Many of these axons cross one another. However, for these experiments, individual, uninterrupted axons of at least 25 μm were used to quantify HSV axonal transport by counting puncta in various segments of axons 0 to 5, 5 to 10,

10 to 15, 15 to 20, and 20 to 25 μm distant from neuronal-cell bodies. A total of 10 to 15 neurons involving four separate experiments were counted for each virus. To determine statistical significance, *P* values were calculated by an unpaired Student's *t* test.

Single-step growth analyses of HSV replication in SK-N-SH neurons. SK-N-SH neurons (plated at 2×10^5 cells/well in 12-well dishes) were grown to near confluence and differentiated with retinoic acid and nerve growth factor for 7 to 10 days. Cells from one well were counted, and triplicate wells were infected with various HSV strains using 5 PFU/cell. The cells and supernatants were combined and harvested at 2, 8, 12, 16, 18, and 24 h; the cells were sonicated; and the titer of the virus was determined using Vero cells.

RESULTS

Production of infections virus in neurons is not reduced by loss of gE/gI or US9. Previous results had demonstrated that HSV gE⁻, gI⁻, and US9⁻ mutants replicated normally in cultured epithelial cells (11, 15, 37, 38). To examine the role of HSV US9 in axonal transport, we used F-US9/GFP, a virus recombinant that has GFP sequences replacing the US9 gene, and F-US9/GFP-R, a repaired version of F-US9 (37). An HSV gE mutant, F-gE/GFP, which has GFP sequences replacing the gE coding sequences, was also described previously (14). F-gE/ GFP produces normal amounts of gD, gI, and US9. Here, we constructed a repaired version of F-gE/GFP, denoted F-gE/ GFP-R, by cotransfecting Vero cells with F-gE/GFP viral DNA and a plasmid (pUC-US7/8) that contains the gE and gI genes (47). Viruses derived from this transfection and lacking GFP were shown to express gE (not shown). It was also important to establish whether gE/gI or US9 reduced HSV replication in cultured neurons. A single-step growth analysis of HSV US9⁻ and gE⁻ viruses was performed using human SK-N-SH neurons infected with each of these viruses at 5 PFU/cell. We observed no differences in the amounts of infectious virus produced by either F-US9/GFP compared with the repaired virus F-US9/GFP-R (Fig. 1A) or F-gE/GFP compared with the repaired virus F-gE/GFP-R (Fig. 1B). Thus, US9 and gE/gI are not required for the production of infectious virus in the cell bodies of infected human neurons.

HSV mutants lacking gE or the gE CT domain display defects in capsid and glycoprotein axonal transport. gE⁻ and gI⁻ mutants are defective in the anterograde spread of HSV from the retina to retinorecipient regions of the brain (12). However, the mechanisms by which gE/gI promotes this anterograde spread are not understood. To begin to address the role of gE/gI in anterograde transport of HSV in axons, we used SK-N-SH neuroblastoma cells that were differentiated with retinoic acid. We previously used these cells in several studies to characterize HSV anterograde transport (42, 43). A substantial fraction of these cells produce neurites or axons of 25 to 75 μm; many of these are bundled, but others that were better isolated and without contacts with other axons were characterized. HSV capsids and glycoprotein-containing vesicles were transported into the axons of these cells with time frames and speeds similar to those of rat dorsal route ganglion (DRG) and rat trigeminal ganglion neurons (42, 43). Specifically, capsids and glycoproteins were transported into axons only after 16 h postinfection (p.i.), and anterograde transport of capsids proceeded at speeds of 0.1 to over 1 μm/s, consistent with fast axonal transport. No sustained retrograde transport was observed, although there was saltatory motion of some capsids (42). Differentiated SK-N-SH neurons were infected
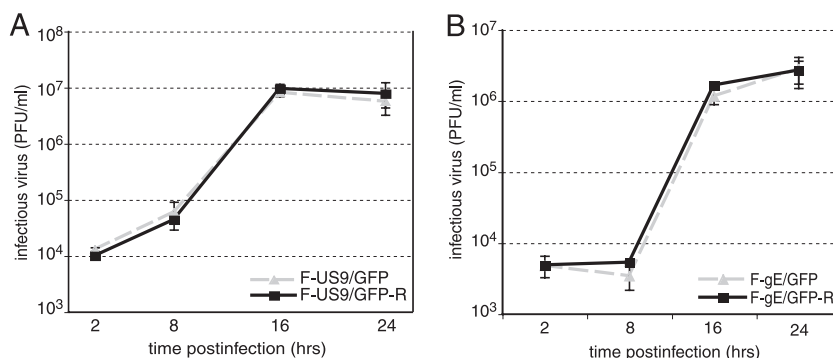
FIG. 1. Replication of HSV US9⁻ and gE⁻ mutants in human neurons. Differentiated SK-N-SH neurons were infected using 5 PFU/cell with either F-US9/GFP (US9⁻) or F-US9/GFP-R (a repaired version of F-US9/GFP) (A) or with F-gE/GFP (gE⁻) or F-gE/GFP-R (a repaired version of F-gE/GFP) (B). At various times, triplicate wells of cells and cell culture supernatants were harvested and sonicated, and the titer of infectious virus was determined using Vero cells. Standard deviations are shown as error bars.

with the gE-null mutant F-gE/GFP and the repaired virus F-gE/GFP-R for 18 h, and the cells were fixed, permeabilized, and simultaneously stained with capsid-specific anti-VP5 (red) and gD anti-glycoprotein (green) antibodies. Numerous capsid- and glycoprotein-specific puncta were observed throughout the lengths of axons following infection with (rescued) F-gE/GFP-R after 18 h of infection (Fig. 2A), consistent with previous observations involving wild-type HSV-infected neurons (43). In contrast, many fewer capsids were detected in axons of (gE-null) F-gE/GFP-infected neurons, especially in segments of axons more distal from neuronal-cell bodies (Fig. 2B). We counted individual capsids in proximal, intermediate, and distal axonal segments of 13 F-gE/GFP-infected neurons and 10 F-gE/GFP-R-infected neurons. There were statistically significant reductions in VP5-stained capsids in proximal and medial axonal segments (0 to 5, 5 to 10, and 10 to 15 μm) and few or no capsids observed in the most distal (20- to 25-μm) axonal segments of F-gE/GFP-infected neurons (Fig. 2B and D). The numbers of gD puncta in proximal (0 to 5 and 5 to 10 μm from the cell body) axon segments of F-gE/GFP-infected neurons were more comparable to those observed in F-gE/GFP-R-infected neurons (Fig. 2B and E). However, in more distal segments (15 to 20 and 20 to 25 μm distant) of F-gE/GFP-infected axons, the numbers of gD puncta were substantially reduced (Fig. 2B and E). Similar quantitative reductions in gB puncta in F-gE/GFP- versus F-gE/GFP-R-infected neurons were observed in intermediate and distal axonal segments (not shown). Moreover, very similar results were obtained with F-gE/GFP- and F-gE/GFP-R-infected rat DRG neurons prepared as described previously (43). We concluded that HSV gE (likely acting in the gE/gI complex) promotes axonal transport of both capsids and glycoproteins. The effects of gE/gI were more profound in capsid transport than in glycoprotein transport, especially in the medial axon segments (Fig. 2D and E, VP5 versus gD puncta in the 5- to 10- or 10- to 15-μm axonal segments). Both capsids and glycoproteins were largely absent from the more distal axonal segments of neurons infected with the gE-null mutant.

The CT domain of gE plays an important role in the sorting of gE/gI to the TGN in epithelial cells, the directed egress of virus particles to epithelial junctions, and epithelial cell-to-cell spread (25, 47). To evaluate whether the gE CT domain was important for axonal transport of capsids or glycoproteins, SK-N-SH neurons were infected with F-gEΔCT, a mutant lacking the gE CT domain, and stained with anti-VP5 capsid antibodies (red) and anti-gD or -gB (green) antibodies. Capsid and gB puncta were quantified in 13 individual F-gEΔCT-infected neurons, and we observed reductions in both capsids and gB in more distal axon segments compared with F-gE/GFP-R-infected neurons (Fig. 2C, D, and E). However, F-gEΔCT had an intermediate phenotype, especially with respect to glycoprotein transport, compared with the gE-null mutant F-gE/GFP and repaired F-gE/GFP-R. Therefore, the gE CT domain contributes to the transport of both glycoproteins and capsids in axons.

Neurons infected with an HSV gI⁻ mutant exhibit defective capsid and glycoprotein anterograde transport. HSV gE functions as a gE/gI heterodimer, with evidence that there is little gE or gI expressed in infected cells that is not part of the gE/gI complex (22, 23). Moreover, it is the gE/gI complex that sorts newly formed virus particles toward epithelial and neuronal junctions, with both gE and gI contributing and with each functioning poorly without the other (12, 24, 25). To test the role of gI in axonal transport, an HSV gI mutant, F-gI/GFP, was constructed by replacing the majority of gI coding sequences with GFP sequences (Fig. 3A). A repaired HSV strain, F-gI/GFP-R, in which gI sequences were restored, was also constructed. The loss of gI was confirmed by immunoprecipitation of gI from radiolabeled F-gI/GFP-infected cells (Fig. 3B). Expression of the immature form of gD was reduced by 50% and that of the mature form of gD was reduced by only 15% in F-gI/GFP-infected cells compared to wild-type HSV-infected cells, and repair of the gI gene restored gD protein expression (Fig. 3C). Since the gD and gI transcripts utilize a single poly(A) site downstream of the gI gene, the decrease in gD expression likely represented reduced stability of gD mRNA caused by replacing gI sequences with GFP sequences. F-gI/GFP could readily infect neurons using 1 PFU/cell, and no fewer infected neurons were observed. Thus, this reduction in gD did not obviously reduce HSV entry, a process entirely dependent upon gD. F-gI/GFP expressed gE normally (Fig. 3D). There was no decreased expression of gD in F-gE/GFP-infected cells (Fig. 3C). Neurons infected with F-gI/GFP (13 individual axons were counted) exhibited markedly reduced
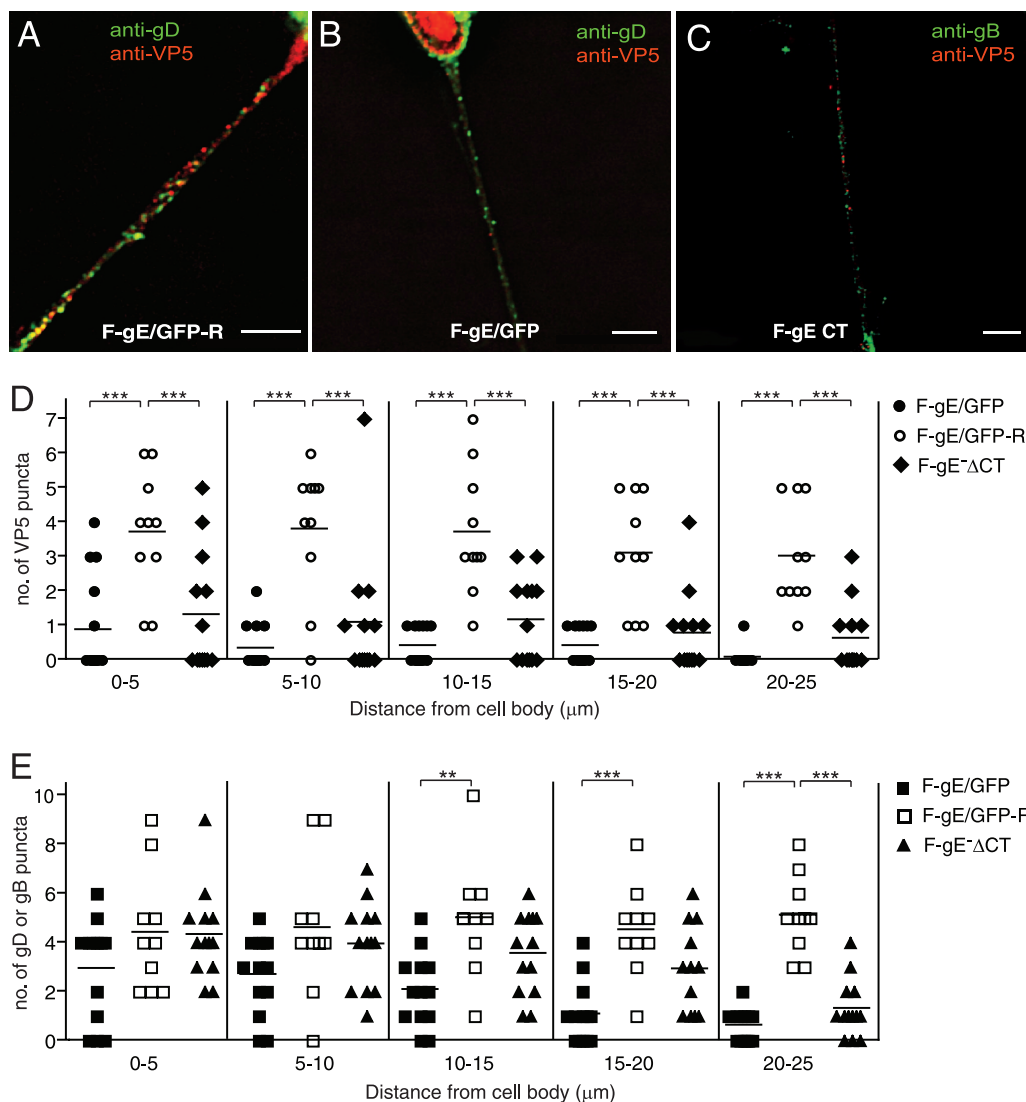
FIG. 2. Axonal transport of capsids and glycoproteins in human neurons infected with HSV gE mutants. SK-N-SH neurons were infected with the repaired F-gE/GFP-R (A), the gE-null mutant F-gE/GFP (B), or a gE mutant lacking the gE CT domain, F-gEΔCT (C), for 18 h; fixed; permeabilized; and stained with mouse anti-VP5 MAb and rabbit anti-gD polyclonal antibodies (A and B) or mouse anti-VP5 MAb and rabbit anti-gB polyclonal antibodies (C), followed by Texas red-conjugated donkey anti-mouse and Cy-5-conjugated anti-rabbit secondary antibodies. Scale bars, 5 μm. Shown is the quantification of VP5 puncta (D) and gB or gD puncta (E) in segments of neuronal axons (0 to 5, 5 to 10, 10 to 15, 15 to 20, or 20 to 25 um) measured from the neuronal cell body. Puncta numbers were obtained from 13 F-gE/GFP-infected, 10 F-gE/GFP-R-infected, and 13 FgE ΔCT-infected neurons involving four independent experiments. Each symbol represents the number of VP5 or glycoprotein puncta observed in the indicated axon segment. Statistically significant values are shown as asterisks, with a *P* value of <0.05 marked as two asterisks and a *P* value of <0.001 marked as three asterisks.

capsid transport in both proximal and distal axons compared with repaired F-gI/GFP-R (10 individual axons were counted) (Fig. 4A, B, and C). Further, there was reduced axonal transport of gB (Fig. 4A, B, and D). Again, gB was observed in proximal segments of axons, but not in distal axons. Our results suggest that gI also substantially contributes to the axonal transport of both capsids and virion glycoproteins, probably acting as part of the gE/gI heterodimer.

US9 promotes anterograde transport of both capsids and glycoproteins. There have been contradictory reports as to how PRV and HSV US9 proteins function in anterograde axonal transport of capsids and glycoproteins in neurons (27, 31, 44).

To characterize the effects of US9 on the transport of capsids and membrane proteins in axons, SK-N-SH neurons were infected with a US9-null HSV strain, F-US9/GFP, or the repaired virus F-US9/GFP-R. The neurons were infected for 18 h, fixed, permeabilized, and stained with capsid-specific anti-VP5 MAb (red) and rabbit anti-gD or -gB antibodies (green). The appearance of capsid puncta in axons was substantially impaired in neurons infected with F-US9/GFP, especially in more distal segments (Fig. 5B, D, and E), compared with the repaired virus (Fig. 5A, C, and E). Axonal transport of both gD (Fig. 5B) and gB (Fig. 5D and F) was also reduced in neurons infected with the US9⁻ mutant, again more promi-
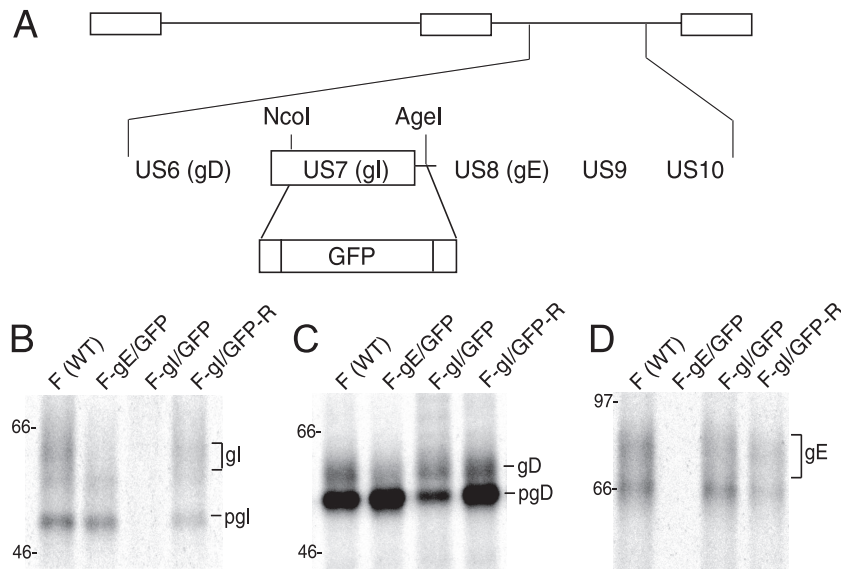
FIG. 3. Construction and characterization of an HSV gI⁻ mutant. (A) Schematic of the HSV unique short component, including the US6 to US10 genes. In F-gI/GFP, the gI (US7) coding sequences between NcoI and AgeI restriction sites were replaced with GFP sequences. A second virus, in which gI sequences were repaired, was produced by cotransfecting Vero cells with F-gI/GFP DNA and a plasmid containing the gE and gI genes. (B to D) R970 cells were infected with either wild-type HSV (WT), F- gE/GFP, F-gI/GFP, or F-gI/GFP-R using 10 PFU/cell for 6 h, and the cells were labeled with [³⁵S]methionine/cysteine for 3 h. gI (B), gD (C), and gE (D) were immunoprecipitated from detergent extracts of the cells using MAb 3104, 3114, or DL6, respectively, and gel electrophoresis was performed. The positions of mature glycoproteins, gI, gD, and gE, and immature forms of glycoproteins, pgI and pgD, and marker proteins of 97, 66, and 46 kDa are indicated.

nently in the more distal segments of axons. The results were quantified by counting puncta in axons of 14 F-US9/GFP-infected neurons and 14 F-US9/GFP-R infected neurons, demonstrating that there were statistically significant differences in the transport of capsids and glycoproteins in medial and distal segments of axons. Similar results were also observed with F-US9/GFP-infected rat DRG neurons (data not shown). We concluded that HSV US9 plays an important role in the transport of both capsids and glycoproteins in neuronal axons.

gE/gI colocalizes with viral-membrane glycoproteins during axonal transport and not with nucleocapsids. Our observations that gE/gI promotes axonal transport of both capsids and membrane glycoproteins raised the question of whether some fraction of gE/gI might colocalize with capsids. Previously, we stained HSV-infected rat DRG neurons and human SK-N-SH neurons with a pool of mouse anti-VP5 capsid MAb and rat anti-gE/gI antibodies in studies that indicated that there was no significant fraction of gE/gI that was transported with capsids (43). To confirm and extend these analyses, we characterized SK-N-SH neurons infected with F-VP26-GFP that expresses the VP26 capsid protein fused to GFP (43) and stained the neurons with rat anti-gE/gI polyclonal antibodies. Transport of HSV capsids into axons is significantly delayed in F-VP26-GFP-infected neurons compared with wild-type HSV-infected neurons (43). Thus, F-VP26-GFP-infected neurons were fixed and stained at 24 h p.i. instead of 18 h p.i. Distinct puncta representing gE/gI (red) and capsids (green) were observed, with very little or no colocalization of gE/gI and capsids (Fig. 6A to C). Of the 200 gE and VP26 puncta counted in six axons, only 4 puncta, or 2%, displayed both red and green signals. As in our previous antibody-staining experiments with these neurons (see Fig. 1 in reference 43), there were instances

in which gE/gI puncta abutted capsid puncta (Fig. 6C). However, higher-magnification images showed that these relatively rare puncta were in no case concentric (Fig. 6C1 and C2).

As an additional means of characterizing the transport of gE/gI in neuronal axons, we characterized whether gE/gI colocalizes with viral glycoproteins using an HSV recombinant, SC16-gD-YFP, that expresses gD fused to yellow fluorescent protein (YFP) (42). Transport of HSV capsids and glycoproteins into axons is also significantly delayed with SC16-gD-YFP (42), and thus, the neurons were characterized at 24 h. We observed extensive colocalization of anti-gE/gI antibodies (red) and gD-YFP puncta (green) (Fig. 7A to C). Quantification of five neuronal axons containing a total of 130 gD-YFP and gE puncta revealed that 128 puncta, or 98% of the total puncta, exhibited overlapping red and green fluorescence. The levels of fluorescence in individual gD-YFP puncta varied considerably, with certain of the gE/gI puncta displaying much lower levels of gD-YFP fluorescence than anti-gE/gI staining. The variable nature of gD-YFP fluorescence is apparently related to proteolytic cleavage that occurs, releasing YFP sequences from gD sequences (42). Extracellular HSV particles vary substantially in the amounts of gD-YFP present in the virion envelope (42). However, virtually all of the gD-YFP puncta with stronger fluorescence displayed staining with anti-gE/gI antibodies. Note that there was a green particle (Fig. 7C) that represented insoluble material not present within the axon. Importantly, gD-YFP clearly showed concentric colocalization with gE/gI staining (Fig. 7C1 and C2). The concentric nature of gE/gI and gD-YFP fluorescence was further confirmed by constructing three-dimensional images involving 11 separate 0.2-μm xy sections stacked along the z axis (see details in Materials and Methods). Rotating these images indicated
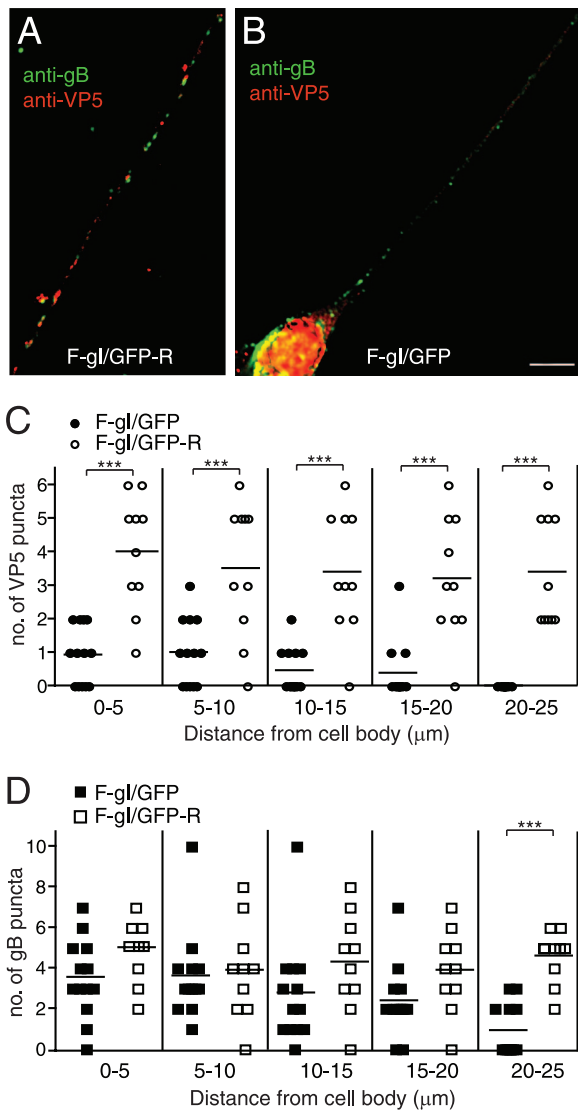
FIG. 4. Axonal transport of capsids and glycoproteins in human neurons infected with the HSV gI[−] mutant. SK-N-SH neurons were infected with the repaired F-gI/GFP-R (A) or the gI[−] mutant F-gI/GFP (B) for 18 h, fixed, permeabilized, and stained with mouse anti-VP5 MAb and rabbit anti-gB polyclonal antibodies, followed by Texas red-conjugated donkey anti-mouse and Cy-5-conjugated anti-rabbit secondary antibodies. Scale bars, 5 μm. (C and D) Quantification of VP5 puncta (C) and gB puncta (D) in different segments of neuronal axons measured from the neuronal-cell body. VP5 or gB puncta were counted in 13 F-gI/GFP-infected and 10 F-gI/GFP-R-infected neurons involving four separate experiments. Each symbol represents the number of puncta present in an individual axonal segment. Statistically significant values are shown as asterisks, with $P < 0.05$ marked as two asterisks and $P < 0.001$ marked as three asterisks.

FIG. 5. Axonal transport of capsids and membrane glycoproteins in human neurons infected with an HSV US9^{−} mutant. Differentiated SK-N-SH neurons were infected with either the repaired F-US9/GFP-R (A and C) or the US9-null mutant F-US9/GFP (B and D) for 18 h, fixed, permeabilized, and stained with mouse anti-VP5 MAb and rabbit anti-gD polyclonal antibodies (A and B) or mouse anti-VP5 MAb and rabbit anti-gB polyclonal antibodies (C and D), followed by Texas red-conjugated donkey anti-mouse and Cy-5-conjugated anti-rabbit secondary antibodies. Scale bars, 5 μm. (E and F) Quantification of VP5 puncta (E) and gB puncta (F) in axonal segments measured from the neuronal-cell body. Puncta were counted in the axons of 13 F-US9/GFP-infected and 13 F-US9/GFP-R-infected neurons involving four independent experiments. Each symbol represents the number of puncta present in an individual axonal segment. Statistically significant values are shown as asterisks, with a P value of <0.05 marked as two asterisks and a P value of <0.001 marked as three asterisks.

that there was always at least 90% overlap of gE/gI and gD-YFP fluorescences. Based on these data and the previous work (43), we concluded that HSV gE/gI is transported in axons in association with gD and the other virion membrane glycoproteins but separately from viral capsids.

HSV US9 associates with capsids being transported in neuronal axons. Given the different observations that have been made with PRV and HSV US9 proteins, it was especially
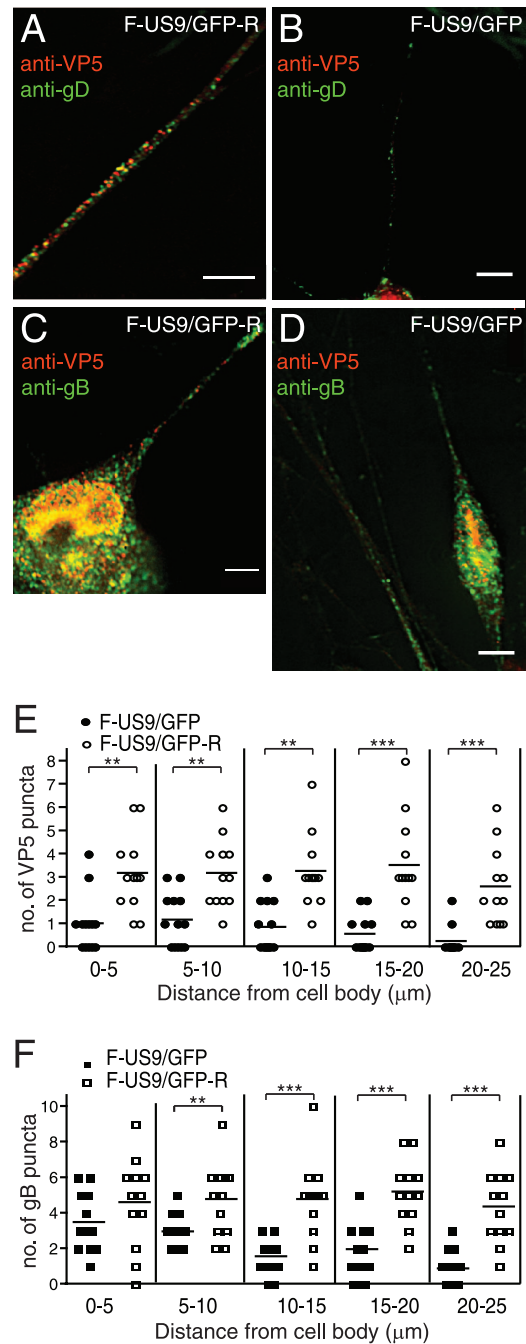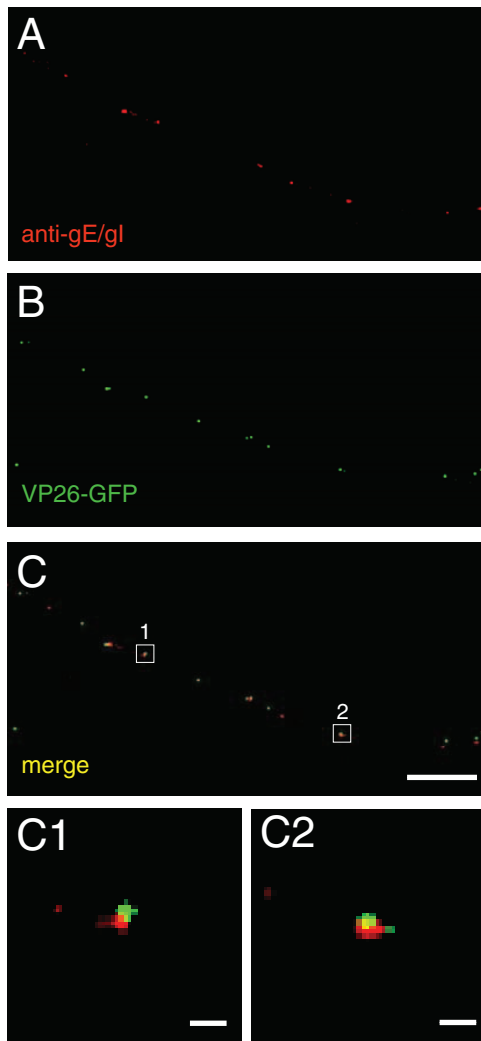
FIG. 6. gE does not associate with capsids in axons of HSV-infected neurons. SK-N-SH neurons were infected with F-VP26-GFP, which expresses a fluorescent capsid protein for 24 h, and then the neurons were fixed, permeabilized, and stained with rat anti-gE/gI polyclonal antibodies, followed by Texas red-conjugated donkey anti-mouse secondary antibodies. Representative results from four independent experiments are shown. (A) Rat anti-gE/gI staining. (B) VP26-GFP fusion protein fluorescence. (C) Merged fluorescence. (C1 and C2) Higher magnifications of the areas boxed in panel C. Scale bars, 5 μm (A to C) and 1 μm (C1 and C2).
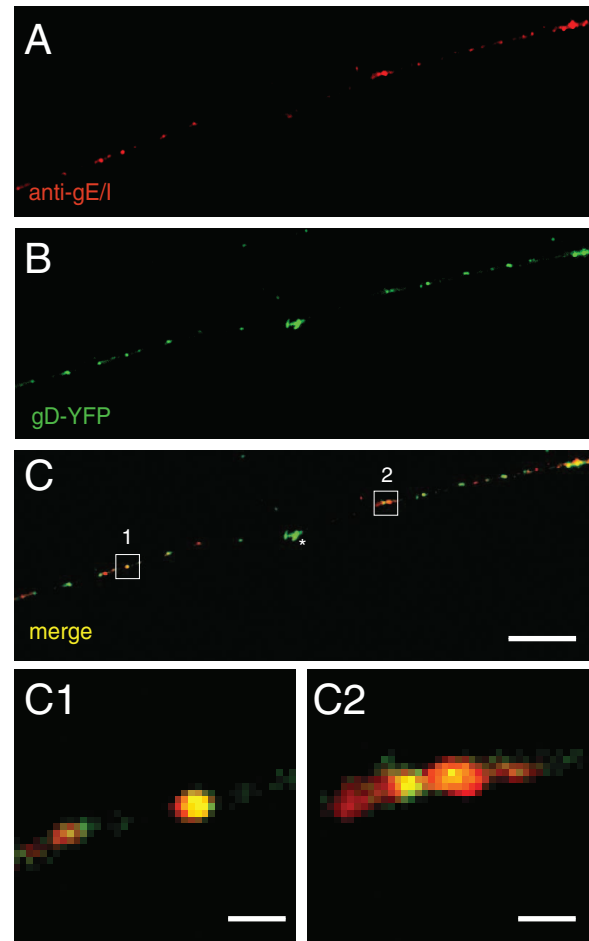

FIG. 7. gE/gI associates with glycoprotein gD in axons of HSV-infected neurons. SK-N-SH neurons were infected with SC16 gD-YFP for 24 h, fixed, permeabilized, and stained with rat anti-gE/gI polyclonal antibodies, followed by Texas red-conjugated donkey anti-mouse secondary antibodies. Representative panels of four independent experiments are shown. (A) Rat anti-gE/gI staining. (B) SC16-gD-YFP fusion protein fluorescence. (C) Merged fluorescence. (C1 and C2) Higher magnifications of the boxed areas in panel C. Scale bars, 5 μm (A to C) and 1 μm (C1 and C2). The star indicates gD-YFP fluorescence associated with a particle that was not present within the axon shown.

important to determine how US9 is distributed in neuronal axons, whether with virion glycoproteins or capsids. We previously described anti-US9 rabbit antibodies produced using a US9-derived peptide (37). Here, these antibodies were adsorbed to uninfected, fixed, permeabilized SK-N-SH neurons and subsequently affinity purified using US9 peptide conjugated onto a matrix. These affinity-purified antibodies did not stain uninfected neurons or neurons infected with the US9-null mutant (not shown). Wild-type HSV-infected SK-N-SH neurons were stained with these anti-US9 antibodies (green) and simultaneously with anti-VP5 MAb (red). The majority of VP5-stained capsids distributed with US9-specific antibodies throughout the entire lengths of axons (Fig. 8A to C), and this

colocalization was concentric (Fig. 8C1 and C2). However, there were also lightly stained US9 puncta (green) that did not discernibly stain with anti-VP5 antibodies (Fig. 8A and B). Quantification of 175 VP5-staining (capsid) puncta in 10 separate axons demonstrated that 81% of these puncta exhibited US9 antibody staining. Again, three-dimensional reconstructions were used to characterize colocalization. In other experiments (not shown), of the 122 puncta that were stained with anti-gD antibodies in seven axons, only 3% also stained with anti-US9 antibodies.

To further characterize the localization of US9 in neuronal axons, we constructed an HSV recombinant, F-US9-HA, that expresses a US9 protein with an insertion of 9 amino acids (directly after the US9 initiation methionine) encoding an influenza virus HA epitope. If the HSV US9 protein is a type II membrane protein with a C-terminal membrane anchor, as is
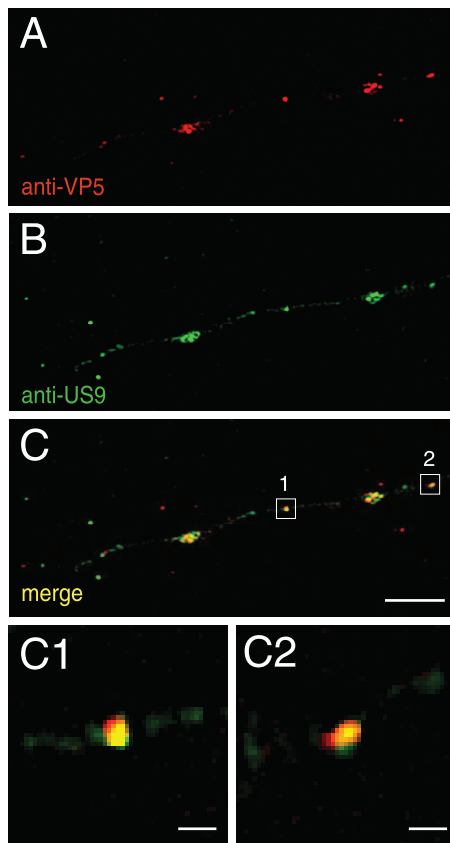
FIG. 8. US9-specific antibodies stain capsid puncta in axons of HSV-infected neurons. SK-N-SH neurons were infected with wild-type HSV for 18 h, fixed, permeabilized, and stained with mouse anti-VP5 MAb and simultaneously with affinity-purified rabbit anti-US9 antibodies, followed by Texas red-conjugated donkey anti-mouse secondary antibodies and fluorescein isothiocyanate-conjugated donkey anti-rabbit secondary antibodies. Panels A to C are representative of three independent experiments. (A) Mouse anti-VP5 staining. (B) Rabbit anti-US9 staining. (C) Merged fluorescence. (C1 and C2) Higher magnifications of the areas boxed in panel C. Scale bars, 5 μm (A to C) and 1 μm (C1 and C2).
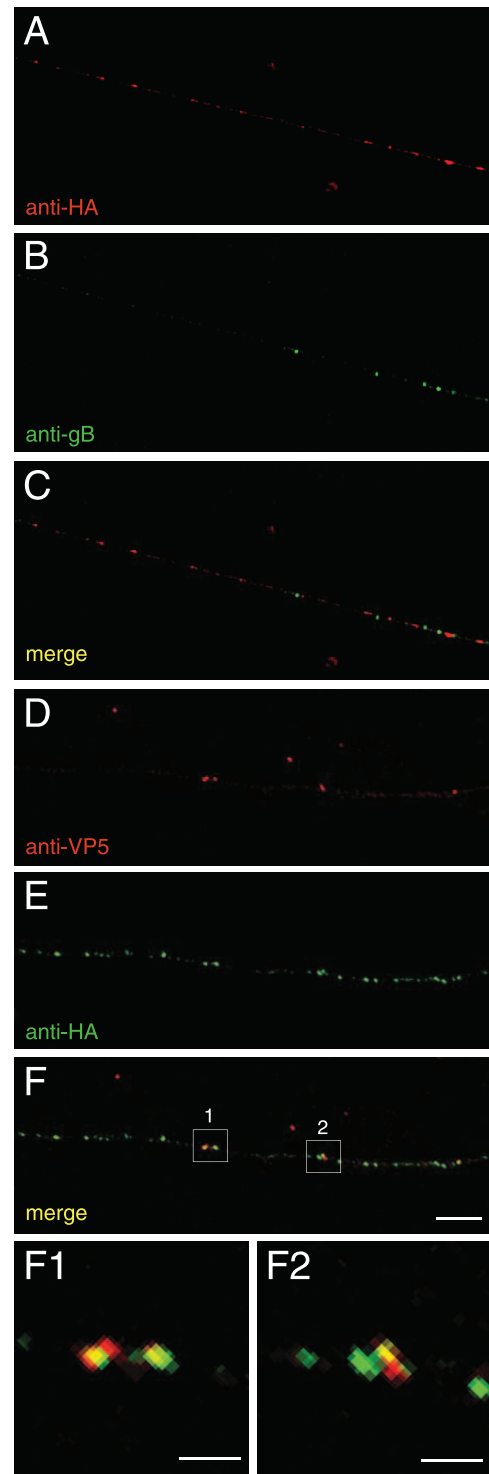

FIG. 9. HA epitope-tagged US9 closely associates with capsids in neuronal axons. SK-N-SH neurons were infected with F-US9-HA for 18 h, fixed, permeabilized, and stained with mouse anti-HA MAb and rabbit anti-gB polyclonal antibodies (A to C) or rabbit anti-HA polyclonal antibodies and mouse anti-VP5 MAb (D to F). Secondary antibodies were Texas red-conjugated donkey anti-mouse secondary antibodies and fluorescein isothiocyanate-conjugated donkey anti-rabbit. The images are representative of three independent experiments. (F1 and F2) High magnifications of axonal segments 1 and 2 in panel F. Scale bars, 5 μm (A to F) and 1 μm (F1 and F2).

clearly the case with PRV US9 (2), then this N-terminal HA epitope should not alter membrane insertion. The HA-tagged HSV US9 was used to replace the GFP sequences in F-US9/GFP, producing a recombinant denoted F-US9-HA. Expression of US9-HA was confirmed by Western blots involving anti-HA MAb and anti-US9 antibodies (data not shown). Capsids and glycoprotein vesicles were transported into axons in normal numbers in F-US9-HA-infected neurons, suggesting that the HA epitope did not compromise US9 function. To determine whether US9 localized with viral glycoproteins, F-US9-HA-infected SK-N-SH neurons were stained with rabbit anti-gB polyclonal antibodies (green) and anti-HA MAb (red) to follow US9. There was very little or no colocalization of gB-containing puncta with US9-HA puncta (Fig. 9A to C). In other experiments, US9-HA was not localized with gD stained with anti-gD polyclonal antibodies (not shown). To determine whether US9 associated with capsids, F-US9-HA-infected neurons were stained with anti-VP5 MAb and rabbit polyclonal anti-HA antibodies. The vast majority of VP5

puncta also stained with US9-HA antibodies (Fig. 9D to F). Those capsid puncta that exhibited HA staining displayed concentric fluorescence, as shown in two-dimensional representations (Fig. 9F1 and F2), as well as in three-dimensional analyses. Note that there were also numerous US9 puncta that did not display anti-VP5 staining, suggesting that US9 is also transported down axons separately from capsids. Therefore, these studies involving epitope-tagged US9 coupled with observations with affinity purified US9-specific antibodies led us to conclude that US9 is transported in neuronal axons in association with capsids. These same capsids were not surrounded by an envelope containing the HSV envelope glycoproteins gB, gD, and gE/gI. Moreover, US9 was not transported in association with the viral envelope glycoproteins gB and gD. However, there was also US9 that was transported in axons without obvious evidence of capsids.

DISCUSSION

Numerous animal studies have demonstrated that HSV gE/gI and US9 play vital roles in promoting virus spread in the nervous system (12, 37, 46). In neurons, these proteins function selectively in anterograde spread, i.e., transport of nascent virus particles from cell bodies to axon termini, and not in retrograde transport of incoming virus particles. However, the molecular mechanisms through which HSV gE/gI and US9 promote anterograde axonal transport are not clear, and there have been inconsistent reports on whether PRV and HSV US9 proteins promote anterograde axonal transport of capsids, glycoproteins, or both (27, 31, 44). To try to better understand how HSV gE/gI and US9 affect anterograde spread, we characterized capsid and glycoprotein transport in cultured human neurons infected with gE⁻, gI⁻, and US9⁻ HSV mutants. Using cultured neurons to characterize axonal transport provides distinct advantages over animal studies, where it is often difficult to tell whether the numbers of viruses entering neurons are the same and whether the effects are specifically on axonal transport or involve spread between cells. For example, HSV gE-null mutants display major defects in virus spread within the retina (involving either retinal epithelial cells or neurons), so that the bolus of virus transported into the optic nerve is markedly reduced. Moreover, spread to the retinorecipient regions of the brain involves not only spread within neurons, but also spread between neurons (12).

HSV mutants lacking gE, gI, or US9 all failed to transport both capsids and viral glycoproteins (gB and gD) normally into axons of human SK-N-SH and rat DRG neurons. Defects in the transport of capsids and glycoproteins were not absolute. There were some capsid and glycoprotein puncta observed in more proximal axons of gE⁻, gI⁻, or US9⁻ HSV-infected neurons, often fewer than were observed with repaired viruses, and markedly decreased numbers of both capsids and glycoproteins in the more distal axon segments. Capsid transport into even proximal regions of axons appeared to be more sensitive to the loss of either gE/gI or US9 than the transport of HSV glycoproteins. These differential effects of gE/gI or US9 mutations on capsid versus glycoprotein transport offer further support for the Separate model for HSV. Our results suggest that HSV gE/gI and US9 both play important roles in axonal transport, and given that there was some transport with single mutants, these proteins likely act in a redundant manner. Our observations are consistent with observations that PRV gE/gI and US9 are important for both capsid and glycoprotein transport (6, 31), although it appears that for PRV, enveloped virions are transported. However, our observations differ from the conclusions drawn by LaVail and colleagues, who suggested that HSV capsids were poorly transported into the optic tract of US9⁻ HSV-infected mice but that glycoproteins were transported normally (27). A close inspection of their data, however, suggested to us that two HSV glycoproteins, gC and gD (analyzed by Western blotting), were reduced in the optic tracts of US9⁻ HSV-infected mice.

gE/gI functions as a heterodimer, and thus, it was not surprisingly to find that HSV mutants lacking either gE or gI exhibited very similar defects in capsid and glycoprotein transport in axons. One might argue that defects in axonal transport with the gI mutant, F-gI/GFP, could be explained by modest reductions in gD expression (the mature form of gD found in the virion envelope was reduced by only 15%). Arguing against effects of gD in this, we saw no obvious reduction in the entry of gI⁻ HSV into neurons, a process requiring gD. Further, it was shown that PRV gD was not required for anterograde spread (8). Moreover, the gI⁻ mutant was phenotypically similar to the gE⁻ mutant, consistent with the notion that the functional complex is the gE/gI heterodimer. Interestingly, F-gEΔCT, a mutant lacking just the gE CT domain, exhibited an intermediate phenotype compared with the gE-null mutant and wild-type HSV. This suggests that the gE CT domain contributes to axonal transport, but also that other domains in gE/gI are also important and can contribute even when the gE CT domain is removed. The gE and gI ET domains may function in this process. Alternatively, the differences between F-gEΔCT and the gE-null mutant might be explained by the effects of gI, which might contribute in the case of F-gEΔCT but not in the absence of the gE-null virus.

HSV gE/gI is clearly an integral membrane protein, a component of cellular membranes and the virion envelope. If one assumes that the Separate model is correct (and all of the evidence for HSV supports this model), it is not difficult to understand how gE/gI might influence axonal transport of virion glycoproteins. Vesicles containing gE/gI, and also the other envelope glycoproteins (gB and gD), might be directed in transport by virtue of the gE and gI CT domain sorting motifs (32, 48). This would be similar to the sorting of HSV gE/gI in epithelial cells (24) and shares elements with the original model proposed for how PRV US9 functions in axons (45). It was suggested that US9 CT sorting sequences act by tethering membrane vesicles (containing envelope glycoproteins) onto microtubule motors that ferry the vesicles to axon tips by mechanisms similar to the transport of synaptic proteins (reviewed in reference 5). More difficult to explain is how a membrane protein such as gE/gI can promote capsid transport (where capsids are transported as unenveloped particles). Previously, we showed that gE/gI stained with polyclonal antibodies was not colocalized with antibody-stained capsids (43). Here, we extended these analyses by characterizing recombinant HSV expressing gD-YFP or VP26-GFP to confirm that gE/gI colocalizes with glycoproteins and not with capsids. These data argue that gE/gI influences the transport of capsids in axons before the capsids enter the axons. HSV gE/gI is
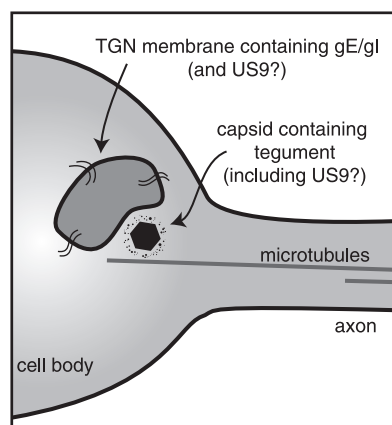
FIG. 10. Model showing how gE/gI and US9 might facilitate the loading of HSV capsids onto microtubules within neuronal-cell bodies. TGN membrane vesicles containing gE/gI and present in neuronal-cell bodies are adjacent to microtubules and serve as platforms for the assembly or loading of HSV tegument-coated capsids onto microtubule motors prior to transport into and down axons. HSV US9 may be a membrane protein and act similarly, or it may be a tegument protein bound to the surfaces of capsids.

concentrated in TGN membranes in epithelial cells (15, 48). TGN membranes containing gE/gI in neurons might physically associate with microtubules and facilitate the loading of HSV capsids and glycoprotein-containing vesicles onto microtubule motors for axonal transport (diagrammed in Fig. 10). It is well established that kinesin motors are anchored on membranes through molecules such as kinectin (reviewed in reference 40). Our observations that the gE CT domain is important for axonal transport fit well with this Loading model because the gE CT domain is important for TGN localization of gE/gI (32, 47, 48). According to the Loading model, gE/gI-modified TGN membranes in the neuronal axon hillock might act as platforms to promote the loading of unenveloped capsids onto microtubule motors and, independently, loading of glycoprotein-containing vesicles onto these motors.

Detailed studies amply defined the PRV US9 protein as a membrane protein (2). Given these results, it is also possible that HSV US9 is a membrane protein, either an integral membrane protein or peripherally bound to membranes. If this is the case, observations that an HSV US9− mutant displayed markedly reduced transport of both capsids and glycoproteins might be explained by the Loading model depicted in Fig. 10. In this case, US9-modified TGN membranes might promote the loading of both capsids and glycoprotein onto microtubule motors for transport into axons. As with other viral processes (14, 16), there is apparently redundancy built into this process, with both gE/gI and US9 contributing to the loading. However, in stark contrast to gE/gI, we found that HSV US9 remained associated with capsids during axonal transport and did not localize with glycoproteins gB and gD. The vast majority (over 80%) of capsids that had been stained with anti-VP5 antibodies also displayed staining with affinity-purified US9-specific antibodies. Capsids were also extensively decorated with US9-HA, detected using anti-HA MAb. In contrast, only 3% of the gD antibody-stained puncta also stained with US9-specific antibodies, and the majority of gB-specific puncta also did not

colocalize with US9-HA puncta. We also found that US9 could be transported in axons independently of capsids, but given observations that US9 puncta almost never contain gB or gD, it is unlikely that HSV glycoproteins are cotransported with US9 in these puncta. However, the salient observation here is that a substantial fraction of US9 was associated with HSV capsids in transit in axons and was not associated with either gB or gD during axonal transport.

Observations that US9 is associated with capsids during axonal transport were surprising if one assumes that HSV US9 is a membrane protein, and considered in terms of the Separate model, in which capsids are transported without an envelope. One potential explanation suggests a refinement of the Separate model in which HSV capsids are associated with (either inside or attached on the outside of) transport vesicles that contain membrane-anchored US9, but not other virion glycoproteins (gB and gD). Such vesicles might be transported in axons separately from vesicles containing virion glycoproteins. Certainly, there have been many descriptions of alphaherpesvirus capsids within membrane structures in axons, as well as an equal number of reports of capsids without obvious membranes, as reviewed in the introduction. Often electron microscopic studies have not indicated whether capsids present within lipid vesicles are enveloped virions, i.e., contain virion glycoproteins.

Alternatively, it is possible that the HSV US9 protein is not exclusively present in membranes, which might imply that HSV US9 differs from PRV US9. The HSV and PRV US9 proteins exhibit 33% amino acid identity and 69% similarity. Early studies of HSV US9 suggested that the protein was a tegument protein found associated with nonenveloped capsids (18) in the nucleus and arguing that US9 is not a membrane protein. More recently, LaVail and colleagues (27) found that HSV US9 antibodies stained cytoplasmic and nuclear membranes, but also unenveloped cytosolic capsids. HSV US9 may be peripherally associated with membranes but might also bind directly or indirectly to capsids that are not enveloped. The UL11 tegument protein extensively localizes onto the surfaces of membranes and also binds other tegument proteins associated with capsids (28, 33). Thus, HSV US9 might be associated with membranes and also bound onto the surfaces of unenveloped capsids in transit in neuronal axons. The observation that US9 is found associated with capsids in axons while gE/gI is not is very intriguing. One could argue that this observation adds further support for the Separate model because antibody-staining experiments that previously demonstrated separate glycoproteins (gE/gI, gB, and gD) and capsids here showed colocalization of US9 with capsids and not the glycoproteins. However, the method of transporting capsids remains unclear, and sorting out the biochemical properties and functions of HSV US9 and gE/gI will be central to a better understanding of neuronal anterograde transport.

REFERENCES

1. **Antinone, S. E., and G. A. Smith.** 2006. Two modes of herpesvirus trafficking in neurons: membrane acquisition directs motion. J. Virol. **80:**11235–11240.
2. **Brideau, A. D., B. W. Banfield, and L. W. Enquist.** 1998. The Us9 gene product of pseudorabies virus, an alphaherpesvirus, is a phosphorylated, tail-anchored type II membrane protein. J. Virol. **72:**4560–4570.
3. **Brideau, A. D., J. P. Card, and L. W. Enquist.** 2000. Role of pseudorabies virus Us9, a type II membrane protein, in infection of tissue culture cells and the rat nervous system. J. Virol. **74:**834–845.
4. **Brideau, A. D., M. G. Eldridge, and L. W. Enquist.** 2000. Directional transneuronal infection by pseudorabies virus is dependent on an acidic internalization motif in the Us9 cytoplasmic tail. J. Virol. **74:**4549–4561.
5. **Brown, A.** 2003. Axonal transport of membranous and nonmembranous cargoes: a unified perspective. J. Cell Biol. **160:**817–821.
6. **Ch'ng, T. H., and L. W. Enquist.** 2005. Efficient axonal localization of alphaherpesvirus structural proteins in cultured sympathetic neurons requires viral glycoprotein E. J. Virol. **79:**8835–8846.
7. **Ch'ng, T. H., and L. W. Enquist.** 2005. Neuron-to-cell spread of pseudorabies virus in a compartmented neuronal culture system. J. Virol. **79:**10875–10889.
8. **Ch'ng, T. H., P. G. Spear, F. Struyf, and L. W. Enquist.** 2007. Glycoprotein D-independent spread of pseudorabies virus infection in cultured peripheral nervous system neurons in a compartment system. J. Virol. **81:**10742–10757.
9. **Collins, W. J., and D. C. Johnson.** 2003. Herpes simplex virus gE/gI expressed in epithelial cells interferes with cell-to-cell spread. J. Virol. **77:**2686–2695.
10. **Diefenbach, R. J., M. Miranda-Saksena, M. W. Douglas, and A. L. Cunningham.** 2008. Transport and egress of herpes simplex virus in neurons. Rev. Med. Virol. **18:**35–51.
11. **Dingwell, K. S., C. R. Brunetti, R. L. Hendricks, Q. Tang, M. Tang, A. J. Rainbow, and D. C. Johnson.** 1994. Herpes simplex virus glycoproteins E and I facilitate cell-to-cell spread in vivo and across junctions of cultured cells. J. Virol. **68:**834–845.
12. **Dingwell, K. S., L. C. Doering, and D. C. Johnson.** 1995. Glycoproteins E and I facilitate neuron-to-neuron spread of herpes simplex virus. J. Virol. **69:**7087–7098.
13. **Dingwell, K. S., and D. C. Johnson.** 1998. The herpes simplex virus gE-gI complex facilitates cell-to-cell spread and binds to components of cell junctions. J. Virol. **72:**8933–8942.
14. **Farnsworth, A., K. Goldsmith, and D. C. Johnson.** 2003. Herpes simplex virus glycoproteins gD and gE/gI serve essential but redundant functions during acquisition of the virion envelope in the cytoplasm. J. Virol. **77:**8481–8494.
15. **Farnsworth, A., and D. C. Johnson.** 2006. Herpes simplex virus gE/gI must accumulate in the trans-Golgi network at early times and then redistribute to cell junctions to promote cell-cell spread. J. Virol. **80:**3167–3179.
16. **Farnsworth, A., T. W. Wisner, M. Webb, R. Roller, G. Cohen, R. Eisenberg, and D. C. Johnson.** 2007. Herpes simplex virus glycoproteins gB and gH function in fusion between the virion envelope and the outer nuclear membrane. Proc. Natl. Acad. Sci. USA **104:**10187–10192.
17. **Feierbach, B., M. Bisher, J. Goodhouse, and L. W. Enquist.** 2007. In vitro analysis of transneuronal spread of an alphaherpesvirus infection in peripheral nervous system neurons. J. Virol. **81:**6846–6857.
18. **Frame, M. C., D. J. McGeoch, F. J. Rixon, A. C. Orr, and H. S. Marsden.** 1986. The 10K virion phosphoprotein encoded by gene US9 from herpes simplex virus type 1. Virology **150:**321–332.
19. **Holland, D. J., M. Miranda-Saksena, R. A. Boadle, P. Armati, and A. L. Cunningham.** 1999. Anterograde transport of herpes simplex virus proteins in axons of peripheral human fetal neurons: an immunoelectron microscopy study. J. Virol. **73:**8503–8511.
20. **Huber, M. T., R. Tomazin, T. Wisner, J. Boname, and D. C. Johnson.** 2002. Human cytomegalovirus US7, US8, US9, and US10 are cytoplasmic glycoproteins, not found at cell surfaces, and US9 does not mediate cell-to-cell spread. J. Virol. **76:**5748–5758.
21. **Husak, P. J., T. Kuo, and L. W. Enquist.** 2000. Pseudorabies virus membrane proteins gI and gE facilitate anterograde spread of infection in projection-specific neurons in the rat. J. Virol. **74:**10975–10983.
22. **Johnson, D. C., and V. Feenstra.** 1987. Identification of a novel herpes simplex virus type 1-induced glycoprotein which complexes with gE and binds immunoglobulin. J. Virol. **61:**2208–2216.
23. **Johnson, D. C., M. C. Frame, M. W. Ligas, A. M. Cross, and N. D. Stow.** 1988. Herpes simplex virus immunoglobulin G Fc receptor activity depends on a complex of two viral glycoproteins, gE and gI. J. Virol. **62:**1347–1354.
24. **Johnson, D. C., and M. T. Huber.** 2002. Directed egress of animal viruses promotes cell-to-cell spread. J. Virol. **76:**1–8.
25. **Johnson, D. C., M. Webb, T. W. Wisner, and C. Brunetti.** 2001. Herpes simplex virus gE/gI sorts nascent virions to epithelial cell junctions, promoting virus spread. J. Virol. **75:**821–833.
26. **Kristensson, K., E. Lycke, M. Roytta, B. Svennerholm, and A. Vahlne.** 1986. Neuritic transport of herpes simplex virus in rat sensory neurons in vitro. Effects of substances interacting with microtubular function and axonal flow [nocodazole, taxol and erythro-9-3-(2-hydroxynonyl)adenine]. J. Gen. Virol. **67:**2023–2028.
27. **LaVail, J. H., A. N. Tauscher, A. Sucher, O. Harrabi, and R. Brandimarti.** 2007. Viral regulation of the long distance axonal transport of herpes simplex virus nucleocapsid. Neuroscience **146:**974–985.
28. **Loomis, J. S., R. J. Courtney, and J. W. Wills.** 2003. Binding partners for the UL11 tegument protein of herpes simplex virus type 1. J. Virol. **77:**11417–11424.
29. **Lycke, E., B. Hamark, M. Johansson, A. Krotochwil, J. Lycke, and B. Svennerholm.** 1988. Herpes simplex virus infection of the human sensory neuron. An electron microscopy study. Arch. Virol. **101:**87–104.
30. **Lycke, E., K. Kristensson, B. Svennerholm, A. Vahlne, and R. Ziegler.** 1984. Uptake and transport of herpes simplex virus in neurites of rat dorsal root ganglia cells in culture. J. Gen. Virol. **65:**55–64.
31. **Lyman, M. G., B. Feierbach, D. Curanovic, M. Bisher, and L. W. Enquist.** 2007. Pseudorabies virus Us9 directs axonal sorting of viral capsids. J. Virol. **81:**11363–11371.
32. **McMillan, T. N., and D. C. Johnson.** 2001. Cytoplasmic domain of herpes simplex virus gE causes accumulation in the trans-Golgi network, a site of virus envelopment and sorting of virions to cell junctions. J. Virol. **75:**1928–1940.
33. **Meckes, D. G., Jr., and J. W. Wills.** 2007. Dynamic interactions of the UL16 tegument protein with the capsid of herpes simplex virus. J. Virol. **81:**13028–13036.
34. **Miranda-Saksena, M., P. Armati, R. A. Boadle, D. J. Holland, and A. L. Cunningham.** 2000. Anterograde transport of herpes simplex virus type 1 in cultured, dissociated human and rat dorsal root ganglion neurons. J. Virol. **74:**1827–1839.
35. **Miranda-Saksena, M., R. A. Boadle, P. Armati, and A. L. Cunningham.** 2002. In rat dorsal root ganglion neurons, herpes simplex virus type 1 tegument forms in the cytoplasm of the cell body. J. Virol. **76:**9934–9951.
36. **Penfold, M. E., P. Armati, and A. L. Cunningham.** 1994. Axonal transport of herpes simplex virions to epidermal cells: evidence for a specialized mode of virus transport and assembly. Proc. Natl. Acad. Sci. USA **91:**6529–6533.
37. **Polcicova, K., P. S. Biswas, K. Banerjee, T. W. Wisner, B. T. Rouse, and D. C. Johnson.** 2005. Herpes keratitis in the absence of anterograde transport of virus from sensory ganglia to the cornea. Proc. Natl. Acad. Sci. USA **102:**11462–11467.
38. **Polcicova, K., K. Goldsmith, B. L. Rainish, T. W. Wisner, and D. C. Johnson.** 2005. The extracellular domain of herpes simplex virus gE is indispensable for efficient cell-to-cell spread: evidence for gE/gI receptors. J. Virol. **79:**11990–12001.
39. **Saksena, M. M., H. Wakisaka, B. Tijono, R. A. Boadle, F. Rixon, H. Takahashi, and A. L. Cunningham.** 2006. Herpes simplex virus type 1 accumulation, envelopment, and exit in growth cones and varicosities in mid-distal regions of axons. J. Virol. **80:**3592–3606.
40. **Sheetz, M. P.** 1996. Microtubule motor complexes moving membranous organelles. Cell Struct. Funct. **21:**369–373.
41. **Smith, G. A., S. P. Gross, and L. W. Enquist.** 2001. Herpesviruses use bidirectional fast-axonal transport to spread in sensory neurons. Proc. Natl. Acad. Sci. USA **98:**3466–3470.
42. **Snyder, A., B. Bruun, H. M. Browne, and D. C. Johnson.** 2007. A herpes simplex virus gD-YFP fusion glycoprotein is transported separately from viral capsids in neuronal axons. J. Virol. **81:**8337–8340.
43. **Snyder, A., T. W. Wisner, and D. C. Johnson.** 2006. Herpes simplex virus capsids are transported in neuronal axons without an envelope containing the viral glycoproteins. J. Virol. **80:**11165–11177.
44. **Tomishima, M. J., and L. W. Enquist.** 2001. A conserved alpha-herpesvirus protein necessary for axonal localization of viral membrane proteins. J. Cell Biol. **154:**741–752.
45. **Tomishima, M. J., G. A. Smith, and L. W. Enquist.** 2001. Sorting and transport of alpha herpesviruses in axons. Traffic **2:**429–436.
46. **Wang, F., W. Tang, H. M. McGraw, J. Bennett, L. W. Enquist, and H. M. Friedman.** 2005. Herpes simplex virus type 1 glycoprotein e is required for axonal localization of capsid, tegument, and membrane glycoproteins. J. Virol. **79:**13362–13372.
47. **Wisner, T., C. Brunetti, K. Dingwell, and D. C. Johnson.** 2000. The extracellular domain of herpes simplex virus gE is sufficient for accumulation at cell junctions but not for cell-to-cell spread. J. Virol. **74:**2278–2287.
48. **Wisner, T. W., and D. C. Johnson.** 2004. Redistribution of cellular and herpes simplex virus proteins from the trans-golgi network to cell junctions without enveloped capsids. J. Virol. **78:**11519–11535.
49. **Zsak, L., F. Zuckermann, N. Sugg, and T. Ben-Porat.** 1992. Glycoprotein gI of pseudorabies virus promotes cell fusion and virus spread via direct cell-to-cell transmission. J. Virol. **66:**2316–2325.